Marine Environmental Research 129 (2017) 229–235

Contents lists available at ScienceDirect

Marine Environmental Research

journal homepage: www.elsevier.com/locate/marenvrev

Carbon assimilation and losses during an ocean acidification mesocosm experiment, with special reference to algal blooms

Nana Liu [a, 1], Shanying Tong [a, 1], Xiangqi Yi [a], Yan Li [a], Zhenzhen Li [a], Hangbin Miao [a], Tifeng Wang [a], Futian Li [a], Dong Yan [a], Ruiping Huang [a], Yaping Wu [b], David A. Hutchins [c], John Beardall [a, d], Minhan Dai [a], Kunshan Gao [a, *]

[a] State Key Laboratory of Marine Environmental Science, Xiamen University, Xiamen, 361102, China
[b] College of Oceanography, Hohai University, Nanjing, 210098, China
[c] Department of Biological Sciences, University of Southern California, Los Angeles, CA, 90089, United States
[d] School of Biological Sciences, Monash University, Clayton, 3800, Victoria, Australia

ARTICLE INFO

Article history:
Received 6 January 2017
Received in revised form
19 May 2017
Accepted 21 May 2017
Available online 27 May 2017

Keywords:
Mesocosm
Elevated pCO_2
Primary production
Carbon losses
Algal blooms
Phytoplankton

ABSTRACT

A mesocosm experiment was conducted in Wuyuan Bay (Xiamen), China, to investigate the effects of elevated pCO_2 on bloom formation by phytoplankton species previously studied in laboratory-based ocean acidification experiments, to determine if the indoor-grown species performed similarly in mesocosms under more realistic environmental conditions. We measured biomass, primary productivity and particulate organic carbon (POC) as well as particulate organic nitrogen (PON). *Phaeodactylum tricornutum* outcompeted *Thalassiosira weissflogii* and *Emiliania huxleyi*, comprising more than 99% of the final biomass. Mainly through a capacity to tolerate nutrient-limited situations, *P. tricornutum* showed a powerful sustained presence during the plateau phase of growth. Significant differences between high and low CO_2 treatments were found in cell concentration, cumulative primary productivity and POC in the plateau phase but not during the exponential phase of growth. Compared to the low pCO_2 (LC) treatment, POC increased by 45.8–101.9% in the high pCO_2 (HC) treated cells during the bloom period. Furthermore, respiratory carbon losses of gross primary productivity were found to comprise 39–64% for the LC and 31–41% for the HC mesocosms (daytime C fixation) in phase II. Our results suggest that the duration and characteristics of a diatom bloom can be affected by elevated pCO_2. Effects of elevated pCO_2 observed in the laboratory cannot be reliably extrapolated to large scale mesocosms with multiple influencing factors, especially during intense algal blooms.

1. Introduction

As a result of human activity, anthropogenic emissions of CO_2 have been increasing from the pre-industrial 280 ppmv to the present-day value of about 400 ppmv, and these will further increase to 800–1000 ppmv by the end of this century according to the Intergovernmental Panel on Climate Change (Pachauri et al., 2014). As a major sink, the ocean has absorbed approximately 30% of anthropologically derived CO_2, leading to ocean acidification (OA), with ocean pH expected to decrease by 0.3–0.4 units by the end of this century (Rhein et al., 2013; Pachauri et al., 2014).

As CO_2 is the substrate of photosynthesis, alterations to the concentration of $[CO_2]_{aq}$ in seawater are known to have significant effects on marine primary producers (Gao et al., 2012; Mostofa et al., 2016). Generally, it is thought that the enhancement of $[CO_2]_{aq}$ will reduce the energy consumption through down-regulation of carbon dioxide concentrating mechanisms (CCMs), and that the saved energy might enhance the growth of phytoplankton (Hopkinson et al., 2011). However, the increase of pCO_2 will be accompanied by a pH decline, which will cause cells to consume more energy to maintain a constant intracellular pH (Suffrian et al., 2011; Bach et al., 2013). Therefore, the impacts of elevated pCO_2 on phytoplankton are complicated in view of the changes in both substrates for photosynthetic and carbonate chemistry.

* Corresponding author.
E-mail address: ksgao@xmu.edu.cn (K. Gao).
[1] These authors contributed to the work equally and should be regarded as co-first authors.

http://dx.doi.org/10.1016/j.marenvres.2017.05.003
0141-1136/

To date, many studies have examined the influence of elevated pCO_2 on marine primary producers, especially diatoms and coccolithophores. Diatoms are important marine primary producers as they contribute nearly half of oceanic productivity, so their responses to elevated pCO_2 are of great significance. Elevated CO_2 associated with decreased pH may result in different responses (positive, neutral and negative effects) in various diatom species (see review by Gao and Campbell, 2014 and literature cited therein). These different results may stem from different experimental designs, such as levels of light and temperature, as well as different species-specific physiology. Coccolithophores are another important phytoplankton group, performing calcification in addition to photosynthetic carbon fixation. The relative capacities of photosynthesis and calcification have considerable influence on the pH around cells and subsequently on global biogeochemical cycles (Zondervan et al., 2002; De Bodt et al., 2010). However, reported results for the effects of elevated pCO_2 on the photosynthetic process of coccolithophores are not consistent (Orr et al., 2005; Langer et al., 2006). Both coccolithophores and diatoms are widespread in the world oceans, and coccolithophore blooms are often observed to occur after those of diatoms (Heimdal et al., 1994; Brown and Yoder, 1994; Brown, 1995). The amounts of fixed carbon and assimilated nitrogen by diatoms and coccolithophores are of general concern regarding future oceanic carbon sequestration and global biogeochemical C and N cycles, since primary production mediates the transformation of CO_2 into organic carbon with variable stoichiometric relationships to other major elements, such as nitrogen (N) and phosphorus (P) (Engel et al., 2013). Due to the presence of the coccoliths in coccolithophores, the ratio of diatoms relative to coccolithophores influences the ratio of organic relative to inorganic carbon in sedimenting particles, which is important for deep-sea carbon storage.

Many studies related to the effects of elevated pCO_2 on phytoplankton have been carried out in small scale laboratory experiments, usually in cultures of less than a litre, maintained under constant light and temperature levels. Although these studies are very important to reveal mechanistic responses to changing seawater carbonate chemistry caused by ocean acidification, the results are difficult to extrapolate to natural dynamic environments. Mesocosms are known to provide a powerful tool to maintain a relatively complex community, which take relevant aspects from “the real world” into account (Riebesell et al., 2013).

Here, we report on a mesocosm experiment conducted to study the influence of elevated pCO_2 on the primary production and biogeochemical cycle of an artificial phytoplankton community, including diatoms and coccolithophores, which had been grown in the laboratory and had been previously examined for their responses to elevated pCO_2. We hypothesized that the effects of elevated pCO_2 on the diatoms and coccolithophores obtained in the laboratory might differ when these species are grown at a large scale under the influence of multiple factors in the sea.

2. Materials and methods

2.1. Experimental setup

The mesocosm experiments were carried out on a floating platform at the Facility for Ocean Acidification Impacts Study of XMU (FOANIC-XMU, 24.52°N, 117.18°E) in Wu Yuan Bay between 22 December 2014 and 24 January 2015 (the day for algae inoculation was set as day 0). Six cylindrical transparent thermoplastic polyurethane (TPU) bags with domes were deployed along the south side of the platform. The width and depth of each mesocosm bag was 1.5 m and 3 m, respectively.

Filtered (0.01 μm, achieved using an ultrafiltration water purifier, MU801-4T, Midea, China) *in situ* seawater was pumped into the six bags simultaneously within 24 h. A known amount of NaCl solution was added into each bag to calculate the exact volume of seawater in the bags, according to the comparison of the salinity before and after salt addition (Czerny et al., 2013). The initial *in situ* pCO_2 was about 650 μatm. To set the low and high pCO_2 levels, we added Na_2CO_3 solution and CO_2 saturated seawater into mesocosm bags to alter the TA (total alkalinity) and DIC (dissolved inorganic carbon) (Gattuso et al., 2010; Riebesell et al., 2013). Subsequently, during the whole experimental process, air at the ambient (400 μatm) and elevated pCO_2 (1000 μatm) concentrations were continuously bubbled into the mesocosm bags using a CO_2 Enricher (CE-100B, Wuhan Ruihua Instrument & Equipment Ltd, China). A flow rate of about 5 L per minute was applied for each bag, and the air was dispersed at the bag's bottom using pre-cleaned airstones.

2.2. Algal strains

Three phytoplankton strains were inoculated into the mesocosm bags, all species at 4×10^4 cells L^{-1}. Both *Phaeodactylum tricornutum* (CCMA 106) and *Thalassiosira weissflogii* (CCMA 102) were obtained from the Center for Collections of Marine Bacteria and Phytoplankton (CCMBP) of the State Key Laboratory of Marine Environmental Science (Xiamen University), the former being originally isolated from the South China Sea (SCS) in 2004 and the other isolated from Daya Bay in the coastal South China Sea. *Emiliania huxleyi* PML B92/11, was originally isolated in 1992 from the field station of the University of Bergen (Raunefjorden; 60°18′N, 05°15′E).

2.3. Measurements of chlorophyll a

Chlorophyll *a* (Chl *a*) was measured using water samples (200 mL-1000 mL) collected every two days at 9 a.m. by filtering onto Whatman GF/F filters (diameter: 25 mm; pore diameter: 0.7 μm). The filters were placed into 5 mL 100% methanol overnight at 4 °C and centrifuged at 5000 g for 10 min. The absorbance of the supernatant (2.5 mL) was measured from 250 to 800 nm using a scanning spectrophotometer (DU 800, Beckman Coulter Inc).

2.4. Primary productivity

The measurement of primary productivity was conducted every two days. Just before sunrise, an 80 mL sample was withdrawn from each bag using a syringe, and divided into four glass scintillation vials for different treatments.

100 μL $NaH^{14}CO_3$ (ICN Radiochemicals, Irvine, CA, USA) containing 5 μCi (0.185 MBq) ^{14}C was added to each glass scintillation vial (20 mL). Vials, covered with a dark neutral net to provide similar light levels as in the bags, were incubated under sunlight with temperature controlled by flowing *in situ* seawater. Over the following 24 h, samples were filtered onto GF/F glass filters every 12 h, and the filters stored at −20 °C. After fuming overnight with concentrated HCl, the membrane samples were dried (50 °C, 6 h) to expel non-fixed labeled carbon (Gao et al., 2007). 4 mL of scintillation cocktail (Hisafe 3, Perkin-Elmer) was added to each vial, then a liquid scintillation counter (Tri-Carb 2800TR, Perkin-Elmer, Waltham, USA) was used to count the radioactivity of fixed ^{14}C.

2.5. C and N measurements

Samples for particulate organic carbon (POC) and particulate organic nitrogen (PON) determination were taken at the same time as those for Chl *a*. Water samples were filtered onto pre-combusted

(450 °C for 5 h) Whatman GF/F filters (25 mm) and stored at −20 °C. After being fumed with HCl for 24 h, filters were analyzed using a Perkin Elmer Series II CHNS/O Analyzer 2400 (Perkin Elmer Waltham, MA).

2.6. Data analyses

The calculation of Chl *a* concentration was according to the equation of Porra (2002), and shown as following:

$$[\text{Chla}]\ (\mu g\ mL^{-1}) = 16.29 \times (A_{665}\text{-}A_{750})\text{-}8.54 \times (A_{652}\text{-}A_{750})$$

A_{652}, A_{665} and A_{750} represent absorption values at wavelengths of 652, 665 and 750 nm, respectively.

The rate of photosynthetic carbon fixation per day was calculated based on the formula of Holm-Hansen and Helbling (1995). The amount of fixed carbon was obtained according to the following equation:

$$\mu mol\ C/L = [(CPM_L\text{-}CPM_D)/Ce] \times I_f \times DIC/A$$

CPM_L represents the amount of radiation fixed in a sample exposed to light (counts per minute) and CPM_D is the amount of radioactive material fixed in the control sample (dark bottle). Ce represents the counting efficiency of the liquid scintillation counter which is obtained through the measurement of ^{14}C standards. I_f is an isotope difference factor (1.06). DIC is the total dissolved inorganic carbon concentration in the medium and A is the activity (in μCi) of added ^{14}C multiplied by 2.2×10^6. The rate of photosynthetic carbon fixation is then calculated as μg C (μg Chl *a*)$^{-1}$ h^{-1}.

One-way ANOVA and Tukey tests as well as two-sample t-tests were carried out to demonstrate the differences between the treatments. ANOVA identified a significant difference with $p < 0.05$.

3. Results

3.1. Growth in the mesocosms consisted of 3 phases

The phytoplankton growth process could be divided into three phases in terms of the variation of Chl *a* concentration (Fig. 1) in the mesocosm experiments. These were i) the logarithmic growth phase (phase I, days 0–15), ii) a plateau phase (phase II, days 15–25, bloom period), and iii) a secondary plateau phase (phase III, days 25–33) attained after a decline in biomass from a maximum in phase II (Fig. 1). The initial chemical parameters of the mesocosm experiment are shown in Supplementary Table S1. The initial dissolved inorganic nitrogen (DIN, including NO_3^-, NO_2^- and NH_4^+) concentrations were 72.0 ± 5.9 μmol L^{-1} for the LC treatment and 74.7 ± 2.8 μmol L^{-1} for the HC treatment. The initial PO_4^{3-} concentrations were 2.6 ± 0.2 μmol L^{-1} and 2.5 ± 0.2 μmol L^{-1} for the LC and HC treatments, respectively. The initial Si concentrations were 38.4 ± 1.8 μmol L^{-1} for the LC treatment and 39.4 ± 0.7 μmol L^{-1} for the HC treatment. We observed significant differences for pCO_2 levels between both CO_2 treatments from day 0–11, but the differences disappeared with the subsequent growth of the phytoplankton (Fig. 2). The nutrient concentrations (dissolved inorganic nitrogen (DIN) and phosphate) in phase II were below or close to the detection limit (Supplementary Table S1), and the values of Chl *a* concentration reached 109.9 and 108.6 μg L^{-1} for the LC and HC treatments, respectively. Although dissolved inorganic nitrogen (NH_4^+, NO_3^-, NO_2^-) and phosphate were depleted, the Chl *a* concentration of both treatments (biomass dominated by *P. tricornutum*) remained constant over days 15–25 (phase II), then declined over the following days. Moreover, the dissolved inorganic carbon (DIC) concentrations in the medium decreased by 119.4 ± 19.4 and 405 ± 101.4 μmol kg^{-1} for the LC and HC treatments, respectively ($p = 0.009$), during phase II (Li et al., unpublished data).

3.2. Algal community composition

E. huxleyi was only found in phase I and its maximal concentration reached 310 cells mL^{-1} according to the results of microscopic inspection (Fig. 3). *T. weissflogii* was found throughout the whole period in each bag, but the maximal concentration was just 8120 cells mL^{-1} which was far less than the concentration of *P. tricornutum*, that had a maximum cell density of about 1.5 million cells mL^{-1} (Fig. 3C). By the time the populations had entered the plateau phase (Phase II), *P. tricornutum* accounted for at least 99% of all the biomass.

Furthermore, the peak of cell concentration for the LC treatment was recorded on day 19 and observed on day 21 for the HC treatment (Fig. 3A). We could not detect any significant enhancement by the elevated pCO_2 due to the large variation in the data. However,

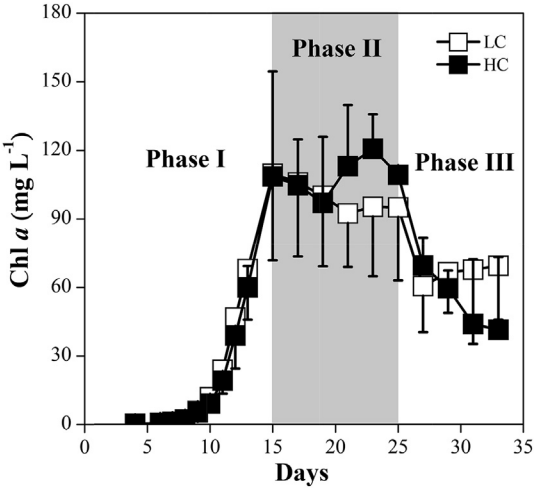

Fig. 1. The average values of Chl *a* concentration in the HC (1000 μatm, solid symbols) and the LC (400 μatm, open symbols) mesocosms (3000 L) during the experiments. According to the changes in levels of Chl *a*, three phases are shown. The shaded area corresponds to Phase II. Data are the means ± SD, n = 3 (triplicate independent mesocosm bags).

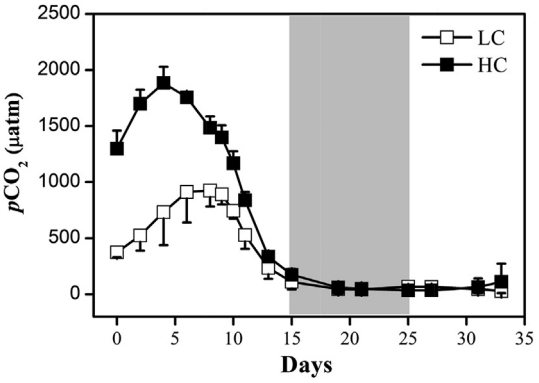

Fig. 2. CO_2 partial pressure (pCO_2) in the HC (1000 μatm, solid symbols) and LC (400 μatm, open symbols) mesocosms (3000 L) during the experiments. Values were obtained from the program CO_2SYS based on the measured pH_T, DIC concentration and other chemical components (such as nutrients). Data are means ± SD, n = 3 (triplicate independent mesocosm bags).

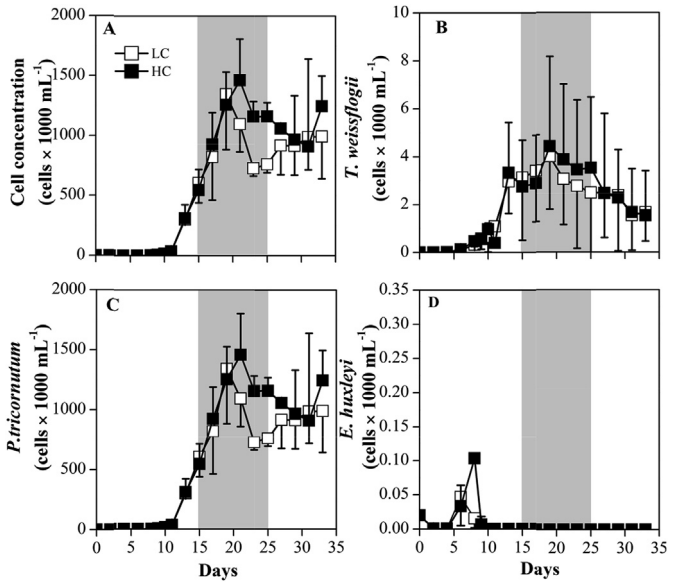

Fig. 3. Cell concentration (cells × 1000 per mL^{-1}). (A) Total cell concentration; (B) cell concentration of *Thalassiosira weissflogii*; (C) cell concentration of *Phaeodactylum tricornutum*; (D) cell concentration of *Emiliania huxleyi*. Open square represents the LC (400 μatm) treatment. Solid square represents the HC (1000 μatm) treatment. The shaded area corresponds to Phase II as shown in Fig. 1. Data are the means ± SD, n = 3 (triplicate independent mesocosm bags).

significant differences between the two pCO_2 treatments were found on day 23 ($p = 0.006$) and 25 ($p = 0.007$) (Fig. 3A), when the cell concentration declined. Although we did not observe any difference between the two pCO_2 treatments during the rapid growth period (days 8–15), a longer period of persistent cell growth and a slower pace in the decrease of population size in phase II were recorded under the HC condition compared to the LC treatment (Fig. 3A).

3.3. Primary productivity and respiration

As shown in Fig. 4, the volume-normalized primary productivity values for 24 h and 12 h incubations increased significantly from day 0–15. A weak positive relationship between primary productivity and Chl *a* concentration was obtained during this period ($R^2 = 0.34$; Pearson's r = 0.59). Notably, the rates of primary productivity increased from 18 to 299 μmol C L^{-1} d^{-1} while nutrient levels declined to below the detection limit. After day 15, the Chl *a* concentrations were almost constant, however, the primary productivity (Fig. 4) decreased drastically, and nutrients (besides silicate and carbon) were also exhausted (except for the 2# bag on day 15, Supplementary Table S1). Although significant changes were recorded for primary productivity and respiration per day as growth proceeded, no significant variation was recorded between the two pCO_2 treatments.

We integrated the primary productivity per litre over different phases to discriminate the amounts of fixed carbon during these periods (Table 1). As shown in Table 1, a significant difference was only observed between the two pCO_2 treatments during the plateau phase for 24 h primary productivity (per litre), which was increased in the elevated pCO_2 treatment by 44%–106%. Using *p* values to demonstrate the statistical significance between both treatments (LC vs HC), the smallest values were recorded in the plateau phase compared to other phases, suggesting that the influence of high pCO_2 on phytoplankton in this experiment was most prominent in the plateau phase. The rates of dark respiration, equating to the difference between 12 h and 24 h primary productivity values, showed no significant difference between the two pCO_2 treatments (Table 1).

3.4. POC and PON

During the growth process in the mesocosm experiment, POC and PON showed slightly different trends. At the initial stage of the experiment, cell concentration was low and the C:N elemental ratio was relatively steady (Fig. 5A, B, C). Along with the increased Chl *a* and cell concentration, PON per litre production rates showed the largest enhancement (93.9 and 97 μmol N L^{-1} day^{-1} for the LC and HC treatments, respectively) during days 10–15. PON per litre peaked at day 17 for both treatments, then values stayed relatively constant over the following days, although a slight decline was seen in the LC treatment. However, the increase of POC per litre did not cease until day 20 for the LC treatment and day 25 for the HC treatment (Fig. 5A). For the initial 15 days, the ratios of POC relative to PON remained at about 5.7 and 5.5 for the LC and HC treatments, respectively ($p = 0.689$) (Fig. 5C), which are a little less than the Redfield ratio (the molar ratio of C, N, and P of marine phytoplankton is about 106:16:1). Over the following days, the ratios of C:N increased significantly due to the continued carbon fixation and steady PON values (Fig. 5A, B, C). During phases II and III, the C:N elemental ratios increased considerably and were always higher than the Redfield ratio (106:16). Although the phytoplankton in the mesocosm bags were under a nutrient-depleted situation after day 15, DIC assimilation continued (Supplementary Fig. S1). Similar maximal values of C:N ratios were recorded from day 15–20 for both pCO_2 treatments. Compared to the low pCO_2 (LC) treatment, the cumulative amount of POC for HC-treated cells during phase II (ΔPOC), increased by 45.8–101.9% ($p = 0.034$) (Fig. 5D), changes similar to the influence of elevated pCO_2 on primary productivity (24 h) in phase II.

4. Discussion

Throughout the experiment, significant changes related to the progress of algal growth were recorded for Chl *a*, POC and PON concentrations. *P. tricornutum* rapidly became the dominant species for all the growth phases, and it maintained high biomass throughout phase II. We found that the impacts of elevated pCO_2 were prominent in this phase, during which ΔPOC of the HC treatment increased by 45.8–101.9% compared to that of the LC treatment. ΔPOC of the HC treatment also increased in parallel to the daily primary productivity. Additionally, a significant difference in cell concentration was detectable between the two pCO_2 treatments during this phase, suggesting that the elevated CO_2 remediates CO_2-limitation during the period of high biomass density.

The influence of exposure to the higher pCO_2 level was prominent in the plateau phase. Considering the fact that during phase I cells entered into a low CO_2 situation with $[CO_2]_{aq}$ of less than 7 μmol L^{-1} (except for 1# bag with 7.0 μmol L^{-1} and 2# bag with 9.1 μmol L^{-1} at day 15, Supplementary Table S1) as well as also being potentially limited by other nutrients (nitrogen and phosphorus) in phase II, active inorganic C uptake and carbon dioxide concentrating mechanisms (CCMs) must have played an important role in the low carbon mesocosms. High C:N ratios of both treatments in phase II might reflect carbon over-consumption by cells grown under nutrient depletion (Taucher et al., 2015) and the accumulation of transparent exopolymer particles (TEP, C:N ratio > 20, Mari et al., 2001). CCMs have been considered to be an effective strategy for maintaining carbon fixation and growth under low CO_2 concentrations (Raven and Beardall, 2014). However, CO_2 enrichment leads to more CO_2 dissolved into the seawater, which

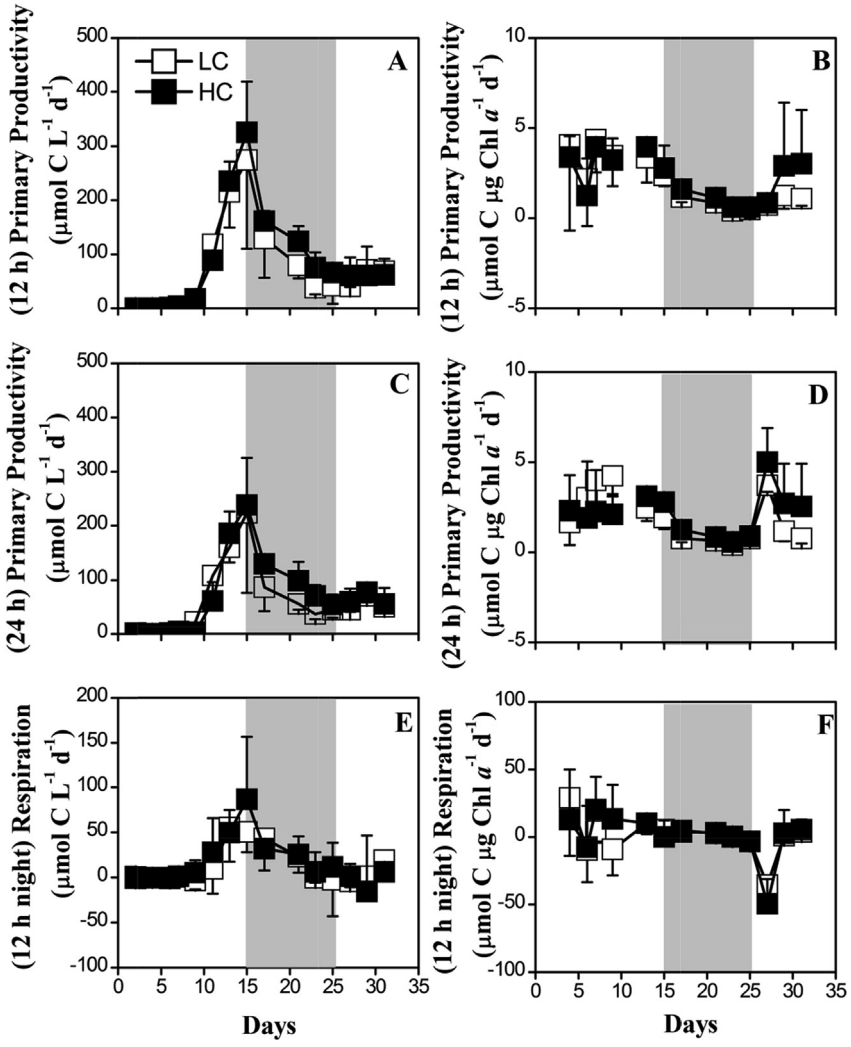

Fig. 4. Primary productivity measured over 12 h and 24 h (including the night period, the difference of daytime and 24 h carbon fixation reflects night period respiration–carbon loss). (A) Primary productivity of 12 h normalized to water volume (L); (B) primary productivity of 12 h normalized to Chl *a*; (C) primary productivity of 24 h normalized to water volume (L); (D) primary productivity of 24 h normalized to Chl *a*; (E) respiration of 12 h night period normalized to water volume (L); (F) respiration of 12 h night period normalized to Chl *a*. Open square represents the LC treatment, and solid square indicates the HC treatment. The shaded area corresponds to Phase II as shown in Fig. 1. Data are the means ± SD, n = 3 (triplicate independent mesocosms bags).

Table 1
Cumulative primary productivity and cumulative dark respiration (μmol C L^{-1}) for different phases. An asterisk represents a significant difference between the two pCO_2 treatments. Data are the means ± SD, n = 3.

Growth Phases	Phase I	Phase II	Phase III
	Logarithmic Growth Phase	Plateau Phase	Second Plateau Phase
	Days 2–15	Days 15–25	Days 25–33
12 h			
Low pCO_2	986 ± 216	1015 ± 492	334 ± 75
High pCO_2	1018 ± 167	1398 ± 93	371 ± 112
p	0.848	0.256	0.657
24 h			
Low pCO_2	811 ± 231	471 ± 154	322 ± 43
High pCO_2	760 ± 194	874 ± 138	381 ± 62
p	0.743	0.013*	0.252
Dark respiration			
Low pCO_2	175 ± 86	544 ± 405	11 ± 68
High pCO_2	258 ± 36	524 ± 49	−10 ± 172
p	0.195	0.934	0.853

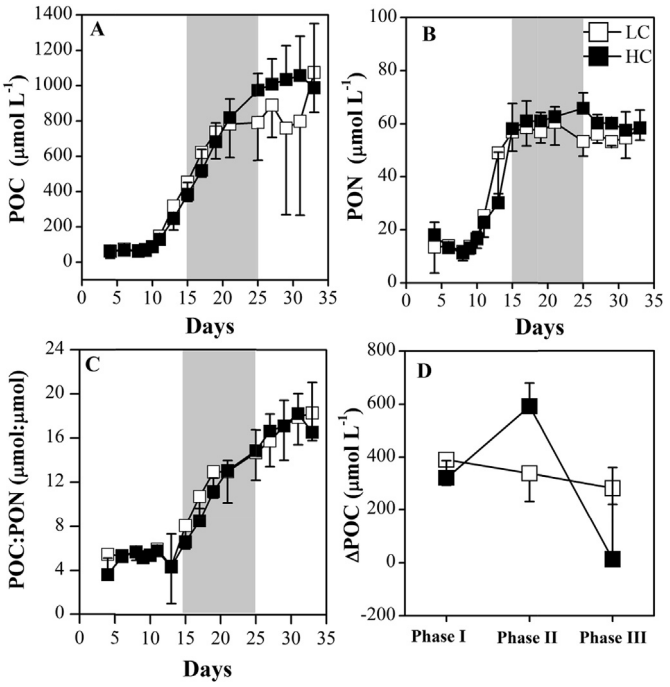

Fig. 5. Contents of particulate organic carbon (POC) and particulate organic nitrogen (PON) per L. (A) POC; (B) PON; (C) The ratio of POC to PON; (D) ΔPOC for the two pCO_2 treatments during three phases. Open square represents the LC treatment, and solid square indicates the HC treatment. The shaded area corresponds to Phase II as shown in Fig. 1. Data are the means ± SD, n = 3.

could provide cells with more $[CO_2]_{aq}$ and reduce diffusive leakage of CO_2 from the cell and cause down-regulation of the CCMs activity (Hopkinson et al., 2011; Taucher et al., 2015). Down-regulation of CCMs activity can save the capital and operation energy costs for their operation, and lead to enhanced carbon fixation or growth (Gao et al., 2012). Higher pCO_2 has been shown to enhance intracellular ATP concentrations for P-replete and P-limited cultured cells (Spungin et al., 2014). Energy saved from the down-regulation of CCMs activity under HC conditions during the logarithmic growth phase of growth might also pave the way for continued cell division and account for the difference of carbon fixation between the two pCO_2 treatments under the nutrient-depleted conditions of phase II (Taucher et al., 2015). In terms of respiratory carbon loss, we did not observe significant differences between the LC and HC mesocosms, which is inconsistent with laboratory findings that HC treatment raised mitochondrial respiration by about 34% in *P. tricornutum* (Wu et al., 2010). Such a discrepancy could be attributed to 1) measuring techniques (^{14}C incorporation vs O_2 consumption) and/or 2) growing conditions (mesocosm vs lab bottles).

Based on data from indoor nutrient-sufficient experiments, the maximum specific growth rate of *T. weissflogii* is about 1.2 d^{-1} (Sugie and Yoshimura, 2016), that of *P. tricornutum* is about 1.2 d^{-1} (Li et al., 2014), and that of *E. huxleyi* is about 0.8–1 d^{-1} (Xing et al., 2015). Calcification and silicification, needed by *E. huxleyi* and *T. weissflogii* respectively, are energy dependent processes. In terms of the competition among the three algae, the capacity of nutrient storage during the nutrient-replete period (luxury consumption) might be another reason for diatoms overwhelmingly outcompeting the coccolithophore (Sommer, 1989). Moreover, *E. huxleyi* has been shown to be more sensitive to excessive light levels compared with *T. weissflogii* (Van de Poll et al., 2007). Silicate was detectable for the whole experimental period, and therefore, was unlikely to be a limiting factor for *T. weissflogii*, despite its larger size and greater investment in frustule structure than *P. tricornutum*. There is a possibility that *P. tricornutum* outcompeted *T. weissflogii* because of its higher surface to volume ratio and/or species specific physiology, which should enhance the efficiency of nutrient uptake and related metabolisms (Johansen, 1991; Raven, 1998; Alessandrade et al., 2007).

Over days 15–25, the cell concentration continued to increase for several days. The stored nutrients in diatom cells might contribute to the biomass increase even after the depletion of nutrients in the surrounding seawater (Goldman et al., 1979; Sommer, 1989). Constant biomass (Chl *a*) (Fig. 1) and increased cumulative primary productivity (Supplementary Fig. S1) were also recorded during phase II when nutrient concentrations fell below the detection limit. These observations might imply a high level of recycling of nutrients in bags, stemming from microbial remineralization (Axler et al., 1981) as well as the powerful capacity of *P. tricornutum* to tolerate nutrient-depleted situations (Gervais and Riebesell, 2001; Li et al., 2012). To scavenge externally available nitrogen and phosphorus, cells entering the stationary-phase might possess more nutrient transporters, such as those for ammonium and phosphorus (Dyhrman et al., 2012; Valenzuela et al., 2012). Alkaline phosphatases are also up-regulated under phosphorus deficiency environment (Dyhrman et al., 2012). As a key pathway for anaplerotic carbon fixation into nitrogenous compounds, the ornithine-urea cycle (OUC) of diatoms can use the ammonia from amino acid decarboxylation to trigger nitrogen reuse, and the OUC may be one of strategies used by diatoms to facilitate rapid recovery from nitrogen depleted conditions (Allen et al., 2011; Valenzuela et al., 2012). Maheswari et al. (2010) reported that elevated pCO_2 level could promote the expression of genes related to OUC. As a function of P deficiency, by-passing phosphorus-dependent glycolytic reactions can lead to the recycling of P and continuous hexose-P conversion (Duff et al., 1989; Theodorou et al., 1991). Therefore, the capacity of *P. tricornutum* to tolerate nutrient-limited situations may be the main reason for the persistence of its high biomass during the plateau phase (phase II).

5. Conclusions

The present work demonstrated that diatoms outcompeted coccolithophores in this coastal water ocean acidification mesocosm experiment, which would be closer to the natural environment and larger scale processes rather than the conditions applied in indoor laboratory studies. Moreover, as the prominent impacts of elevated pCO_2 on DIC uptake were only found in the bloom period, we suggest that more attention should be paid to the stationary phase dynamics in future studies. This phenomenon shows that elevated pCO_2 can enhance marine primary productivity and could lead to much more carbon sequestration during the late stages of diatom blooms in the future. The outcome for phytoplankton communities will depend on the sensitivities of the different component species to increased pCO_2 levels, thus, further work is needed to develop a clear picture of the function of OA on algae bloom events in the future high CO_2 oceans.

Acknowledgements

This study was supported by National Natural Science Foundation (41430967), the national key research programs (2016YFA0601400), NSFC- Shandong Joint Fund for Marine Ecology and Environmental Sciences (no. U1606404).

Experimental design mainly based on KSG, YPW and MHD; NNL measured photosynthesis, respiratory carbon loss and other related parameters and drafted the paper. SYT measured POC/PON and

drafted the introduction of this paper. XQY, RPH, DY, HBM, ZZL, TFW, FTL contributed to cell counting and photosynthetic carbon fixation. YL measured the chemistry parameters. KSG, JB and DH were involved in data analysis and paper writing.

Appendix A. Supplementary data

Supplementary data related to this article can be found at http://dx.doi.org/10.1016/j.marenvres.2017.05.003.

References

Axler, R.P., et al., 1981. The importance of regenerated nitrogen to phytoplankton productivity to phytoplankton productivity in a subalpine lake. Ecology 62 (2), 345–354. http://dx.doi.org/10.2307/1936709.

Alessandrade, M., et al., 2007. Genetic and phenotypic characterization of *Phaeodactylum tricornutum* (Bacillariophyceae) accessions. J. Phycol. 43, 992–1009. http://dx.doi.org/10.1111/j.1529-8817.2007.00384.x.

Allen, A.E., et al., 2011. Evolution and metabolic significance of the urea cycle in photosynthetic diatoms. Nature 473, 203–207. http://dx.doi.org/10.1038/nature10074.

Bach, L.T., et al., 2013. Dissecting the impact of CO_2 and pH on the mechanisms of photosynthesis and calcification in the coccolithophore *Emiliania huxleyi*. New Phytol. 199, 121–134. http://dx.doi.org/10.1111/nph.12225.

Brown, C.W., Yoder, J.A., 1994. Coccolithophorid blooms in the global ocean. J. Geophys. Res. 99, 7467. http://dx.doi.org/10.1029/93JC02156.

Brown, C.W., 1995. Global distribution of coccolithophore blooms. Oceanography 8, 59–60.

Czerny, J., et al., 2013. Technical note: A simple method for air–sea gas exchange measurements in mesocosms and its application in carbon budgeting. Biogeosciences 10, 1379–1390. http://dx.doi.org/10.5194/bg-10-1379-2013.

De Bodt, C., et al., 2010. Individual and interacting effects of pCO_2 and temperature on *Emiliania huxleyi* calcification: study of the calcite production, the coccolith morphology and the coccosphere size. Biogeosciences 7, 1401–1412. http://dx.doi.org/10.5194/bg-7-1401-2010.

Duff, S.M., et al., 1989. Phosphate starvation inducible bypasses of adenylate and phosphate dependent glycolytic enzymes in Brassica nigra suspension cells. Plant Physiol. 90, 1275–1278. http://dx.doi.org/10.1104/pp.90.4.1275.

Dyhrman, S.T., et al., 2012. The transcriptome and proteome of the diatom *Thalassiosira pseudonana* reveal a diverse phosphorus stress response. PLoS One 7, e33768. http://dx.doi.org/10.1371/journal.pone.0033768.

Engel, A., et al., 2013. CO_2 increases ^{14}C-primary production in an Arctic plankton community. Biogeosciences 10, 1291–1308. http://dx.doi.org/10.5194/bg-10-1291-2013.

Gattuso, J.-P., et al., 2010. Approaches and tools to manipulate the carbonate chemistry. In: Riebesell, U., et al. (Eds.), Guide to Best Practices in Ocean Acidification Research and Data Reporting. Office for Official Publications of the European Communities, Luxembourg, pp. 41–52.

Gao, K.S., et al., 2007. Solar UV radiation drives CO_2 fixation in marine phytoplankton: a double-edged sword. Plant Physiol. 144, 54–59. http://dx.doi.org/10.1104/pp.107.098491.

Gao, K.S., et al., 2012. Rising CO_2 and increased light exposure synergistically reduce marine primary productivity. Nat. Clim. Change 2, 519–523. http://dx.doi.org/10.1038/NCLIMATE1507.

Gao, K.S., Campbell, D.A., 2014. Photophysiological responses of marine diatoms to elevated CO_2 and decreased pH: a review. Funct. plant Biol. 41, 449–459. http://dx.doi.org/10.1071/FP13247.

Gervais, F., Riebesell, U., 2001. Effect of phosphorus limitation on elemental composition and stable carbon isotope fractionation in a marine diatom growing under different CO_2 concentrations. Limnol. Oceanogr. 46, 497–504. http://dx.doi.org/10.4319/lo.2001.46.3.0497.

Goldman, J.C., et al., 1979. Growth rate influence on the chemical composition of phytoplankton in oceanic waters. Nature 279, 210–215. http://dx.doi.org/10.1038/279210a0.

Heimdal, B., et al., 1994. The 1992 Norwegian *Emiliania huxleyi* experiment. An overview. Sarsia 79, 285–290. http://dx.doi.org/10.1080/00364827.1994.10413560.

Holm-Hansen, O., Helbling, E., 1995. Técnicas para la medición de la productividad primaria en el fitoplancton. In: Alveal, K., et al (Eds.), Manual de métodos ficológicos. Universidad de Concepción, Concepción, pp. 329–350.

Hopkinson, B.M., et al., 2011. Efficiency of the CO_2-concentrating mechanism of diatoms. PNAS 108, 3830–3837. http://dx.doi.org/10.1073/pnas.1018062108.

Johansen, J.R., 1991. Morphological variability and cell wall composition of *Phaeodactylum tricornutum* (Bacillariophyceae). Gt. Basin Nat. 51, 310–315.

Langer, G., et al., 2006. Species-specific responses of calcifying algae to changing seawater carbonate chemistry. Geochem. Geophys. Geosystems 7. http://dx.doi.org/10.1029/2005GC001227.

Li, W., et al., 2012. Interactive effects of ocean acidification and nitrogen-limitation on the diatom *Phaeodactylum tricornutum*. PLoS One 7, e51590. http://dx.doi.org/10.1371/journal.pone.0051590.

Li, Y.H., et al., 2014. Light-modulated responses of growth and photosynthetic performance to ocean acidification in the model diatom *Phaeodactylum tricornutum*. PLoS One 9, e96173. http://dx.doi.org/10.1371/journal.pone.0096173.

Maheswari, U., et al., 2010. Digital expression profiling of novel diatom transcripts provides insight into their biological functions. Genome Biol. 11, R85. http://dx.doi.org/10.1186/gb-2010-11-8-r85.

Mari, X., et al., 2001. Non-Redfield C: N ratio of transparent exopolymeric particles in the northwestern Mediterranean Sea. Limnol. Oceanogr. 46, 1831–1836. http://dx.doi.org/10.4319/lo.2001.46.7.1831.

Mostofa, K.M.G., et al., 2016. Reviews and Syntheses: ocean acidification and its potential impacts on marine ecosystems. Biogeosciences 13, 1767–1786. http://dx.doi.org/10.5194/bg-13-1767-2016.

Orr, J.C., et al., 2005. Anthropogenic ocean acidification over the twenty-first century and its impact on calcifying organisms. Nature 437, 681–686. http://dx.doi.org/10.1038/nature04095.

Pachauri, R.K. et al. 2014. Climate Change 2014: Synthesis Report. Contribution of Working Groups I, II and III to the Fifth Assessment Report of the Intergovernmental Panel on Climate Change.

Porra, R.J., 2002. The chequered history of the development and use of simultaneous equations for the accurate determination of chlorophylls a and b. Photosynth. Res. 73, 149–156. http://dx.doi.org/10.1023/A:1020470224740.

Raven, J., 1998. The twelfth Tansley Lecture. Small is beautiful: the picophytoplankton. Funct. Ecol. 12, 503–513. http://dx.doi.org/10.1046/j.1365-2435.1998.00233.x.

Raven, J., Beardall, J., 2014. CO_2 concentrating mechanisms and environmental change. Aquat. Bot. 118, 24–37. http://dx.doi.org/10.1016/j.aquabot.2014.05.008.

Rhein, M., et al., 2013. Chapter 3, Observations: Oceans, in IPCC 2013, Climate Change 2013: The Physical Science Basis. Cambridge Univ Press, Cambridge, UK. Working Group I Contribution to the IPCC 5th Assessment Report.

Riebesell, U., et al., 2013. Technical Note: a mobile sea-going mesocosm system-new opportunities for ocean change research. Biogeosciences 10, 1835–1847. http://dx.doi.org/10.5194/bg-10-1835-2013.

Sommer, U., 1989. The role of competition for resources in phytoplankton succession. In: Plankton Ecology. Springer, pp. 57–106. http://dx.doi.org/10.1007/978-3-642-74890-5_3.

Spungin, D., et al., 2014. *Trichodesmium*'s strategies to alleviate P-limitation in the future acidified oceans. Environ. Microbiol. 16 (6), 1935–1947. http://dx.doi.org/10.1111/1462-2920.12424.

Suffrian, K., et al., 2011. Cellular pH measurements in *Emiliania huxleyi* reveal pronounced membrane proton permeability. New Phytol. 190, 595–608. http://dx.doi.org/10.1111/j.1469-8137.2010.03633.x.

Sugie, K., Yoshimura, T., 2016. Effects of high CO_2 levels on the ecophysiology of the diatom *Thalassiosira weissflogii* differ depending on the iron nutritional status. ICES J. Mar. Sci. 73, 680–692. http://dx.doi.org/10.1093/icesjms/fsv259.

Taucher, J., et al., 2015. Combined effects of CO_2 and temperature on carbon uptake and partitioning by the marine diatoms *Thalassiosira weissflogii* and *Dactyliosolen fragilissimus*. Limnol. Oceanogr. 3, 901–919. http://dx.doi.org/10.1002/lno.10063.

Theodorou, M.E., et al., 1991. Effects of phosphorus limitation on respiratory metabolism in the green alga *Selenastrum minutum*. Plant Physiol. 95, 1089–1095. http://dx.doi.org/10.1104/pp.95.4.1089.

Valenzuela, J., et al., 2012. Potential role of multiple carbon fixation pathways during lipid accumulation in *Phaeodactylum tricornutum*. Biotechnol. Biofuels 5, 40. http://dx.doi.org/10.1186/1754-6834-5-40.

Van de Poll, W.H., et al., 2007. Acclimation to a dynamic irradiance regime changes excessive irradiance sensitivity of *Emiliania huxleyi* and *Thalassiosira weissflogii*. Limnol. Oceanogr. 52, 1430–1438. http://dx.doi.org/10.4319/lo.2007.52.4.1430.

Wu, Y., et al., 2010. CO_2-induced seawater acidification affects physiological performance of the marine diatom *Phaeodactylum tricornutum*. Biogeosciences 7, 2915–2923. http://dx.doi.org/10.5194/bg-7-2915-2010.

Xing, T., et al., 2015. Response of growth and photosynthesis of *Emiliania huxleyi* to visible and UV irradiances under different light regimes. Photochem. Photobiol. 91, 343–349. http://dx.doi.org/10.1111/php.12403.

Zondervan, I., et al., 2002. Effect of CO_2 concentration on the PIC/POC ratio in the coccolithophore *Emiliania huxleyi* grown under light-limiting conditions and different daylengths. J. Exp. Mar. Biol. Ecol. 272, 55–70. http://dx.doi.org/10.1016/S0022-0981(02)00037-0.